# BAYESIAN TRACKING FOR BLOOD VESSEL DETECTION IN RETINAL IMAGES

*Yi Yin, Mouloud Adel, Mireille Guillaume, and Salah Bourennane*

Institut Fresnel, UMR-CNRS 6133, Ecole Centrale Marseille, Université Paul Cézanne
Domaine Universitaire de Saint-Jérôme, 13397, Marseille, France
email: yi.yin@fresnel.fr

## ABSTRACT

A new statistical-based tracking method is proposed for the detection of blood vessels in retinal images. Our algorithm adopts a statistic sample scheme to estimate the candidate edge points of local blood vessel. This sampling scheme combines local grey level profile and the vessel geometric properties, which improves the accuracy and robustness of the tracking process. Edge points of blood vessels are detected iteratively based on a Bayesian approach with the Maximum *a posteriori* (MAP) Probability criterion. Evaluation of our algorithm is presented on both synthetic and real retinal images.

## 1. INTRODUCTION

The early diagnosis of several pathologies, and indicators for the presence of a wide range of diseases, such as arterial hypertension, arteriosclerosis or diabetic retinopathy could be achieved by analyzing vascular structures. For many clinical investigations, vessel segmentation is becoming a prerequisite for the analysis of vessel parameters such as tortuosity and variation of the vessel width along the vessel. An extensive research has been devoted to vessel extraction in medical images using different types of approaches. A major review of these methods can be found in [1]. Most of the work on retinal image segmentation can be categorized into three approaches: those based on line or edge detectors with boundary tracing [2], [3], those based on matched filters, either 1-D profile matching with vessel tracking and local thresholding [4–7] or 2-D matched filters [8–10], and those supervised methods which require manually labeled images for training [11], [12]. A vessel tracking method based on Bayesian theory was proposed in [13], [14], which was in an initial stage of development. It needed some improvements like modelling the blood vessel more accurately and handling different configurations of the vessel.

In this paper, we present an improved tracking algorithm based on our previous work. We use a photometric correction before tracking, which improves the robustness against noise. A semi-ellipse search window is used during the tracking process. Sectional grey level profile of the blood vessel is approximated more appropriately as a Gaussian model.

## 2. METHOD DESCRIPTION

Retinal images such as retinal angiograms often suffer from shading, which may cause measurement error. A photometric correction is used to remove shading before tracking. We estimate the shading through an iterative polynomial interpolation procedure [15]. An example of retinal image, corresponding shading and corrected image are shown in Fig.1.

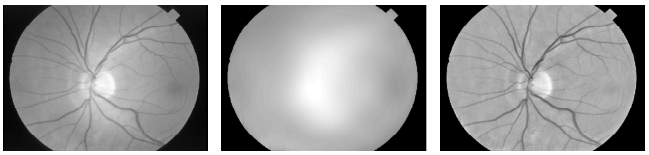

(a) Retinal image (b) Extracted background (c) Corrected image

Figure 1: Example of an retinal angiogram.

The proposed tracking method is applied after photometric correction. Tracking process starts from an initial point, which is determined manually by the user. Edge points are detected iteratively using local statistical parameters calculated on grey levels and information obtained in previous iterations. At each iteration, a statistical sample is used to get the information of local grey levels. A branch detection scheme is performed at each iteration to find if there is a bifurcation at current detecting area. All the branches found are treated as new blood vessels to be detected later. The tracking process stops when all the blood vessels are detected.

### 2.1 Extraction of the statistical sample

In this study, vessel's structures are categorized into three types: normal, bifurcation and crossing. Normal case is regarded as the situation in which only a single vessel exists in current research region. The case of bifurcation means that one single vessel is divided into two branches. A crossing case is described when one vessel overlaps another. The proposed algorithm can detect different structures and the tracking process varies accordingly.

At a given step, new edge points are assumed to be located on a semi-ellipse (see Fig.2) which is defined to be centered on local center point and heading towards current vessel direction. This semi-ellipse can be regarded as a search window restricting the range of possible locations of new edge points. At iteration $k$, we select $N_k$ points which are numbered from 1 to $N_k$ on semi-ellipse $C_k$ as illustrated in Fig.2 (a). $O_k$ and $\overrightarrow{D_k}$ are local center point and vessel direction respectively. A configuration $\chi$ is defined by a set of edge point candidates. Only two points are needed to define a normal configuration. They are assumed to be the $m^{th}$ and $n^{th}$ points on $C_k$ ($1 < m < n < N_k$) and correspond to two diametrically opposite vessel edge points. For this normal configuration, $M_i$ ($i \in [1, N_k]$), the $i^{th}$ point on $C_k$, is assumed to belong to the blood vessel if $i \in [m, n]$ or to the background if $i \in [1, m[ \bigcup ]n, N_k]$.

For a bifurcation configuration, four interface points are needed to describe the edge points of two branches. Six interface points are needed for the crossing configuration. Two of them are considered as the next edge points of the same

 ISSN 2076-1465 

vessel, while the other four points are considered as the edge points of another vessel which is over or under the current one. These types of configurations are illustrated in Fig.2.

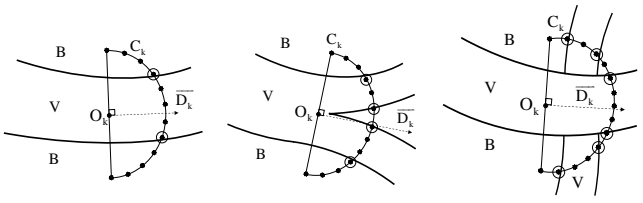


(a) Normal (b) Bifurcation (c) Crossing

Figure 2: Three types of configurations: B means background and V means blood vessel

In order to deal with the complicated features of retinal blood vessel, the semi-ellipse should be self-adapting. For example, when vessel's diameter increases, the semi-ellipse would be enlarged in order to cover the potential position of new edge point. Minor axis of the ellipse which is parallel to local vessel's direction could denote the look-ahead distance. To make the algorithm more robust to curve changes, minor axis is proposed to be adaptive to the vessel's curvature.

At iteration $k$, as shown in Fig.3, the major axis $a_k$ of semi-ellipse $C_k$ is perpendicular to $\overrightarrow{D_k}$ while its minor axis $b_k$ is parallel to it. Let $\theta_k$ stands for the angle between current and previous directions: $\theta_k = (\overrightarrow{D_{k-1}}, \overrightarrow{D_k})$. $\theta_k$ provides the information of local vessel's curvature. Parameter $a_k$ and $b_k$ can be obtained as:

$$\begin{cases} a_k = \alpha d_k \\ b_k = \beta(\pi - \theta_k) d_k \end{cases} \tag{1}$$

where $\alpha$, $\beta$ are constant factors, $d_k$ is local vessel's diameter. In this study, $\alpha$ was set to be 2 which is the best value based on simulated results. $\beta$ is assigned as $1/\pi$ so that the magnitude of the step distance is not more than the vessel's diameter.

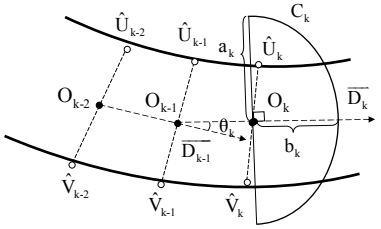


Figure 3: Dynamic search window

## 2.2 Tracking process

In practice, two initial edge points $\hat{U}_1$ and $\hat{V}_1$ are chosen manually diametrically opposed on the interested blood vessel. Initial tracking direction $\overrightarrow{D_1}$ is manually set along local direction of blood vessel. Meanwhile, three areas are selected surrounding the initial point: one inside and two outside the blood vessel. The selected areas are used to calculate the initial statistical parameters of local noise. A source-list stores all the initial information obtained by the user at the initialization or by the algorithm when new branches are identified.

The tracking process of a vessel launches from loading initial data from the source-list. During the tracking process, local blood vessel at iteration $k$ can be described by three parameters: edge points $\hat{U}_k$, $\hat{V}_k$, center point $O_k$, direction $\overrightarrow{D_k}$ (see Fig.3). A semi-ellipse $C_k$ is centered on $O_k$ and heading towards $\overrightarrow{D_k}$. We consider all the possible configurations obtained on $C_k$. Based on the Maximum a posterior (MAP) criterion within the frame of Bayesian theory, the best estimate of the blood vessel is obtained by the configuration $\hat{\chi}$ which has the maximum probability. If $\hat{\chi}$ is a normal configuration, the two points on $C_k$ used to define $\hat{\chi}$ are regarded as next edge points $\hat{U}_{k+1}$, $\hat{V}_{k+1}$ respectively. Next center point $O_{k+1}$ is considered as the middle point of $[\hat{U}_{k+1},\hat{V}_{k+1}]$. New direction $\overrightarrow{D_{k+1}}$ heads towards $\overrightarrow{O_k O_{k+1}}$. This tracking process of current vessel stops when the vessel ends or a bifurcation or crossing configuration is found. When new diameter $d_{k+1}$, $d_{k+1} = |\hat{U}_{k+1}\hat{V}_{k+1}|$, is too small, that is less than one pixel in this study, it means the end of the blood vessel is detected. When a bifurcation or crossing configuration is detected, new branches will be stored in the source-list as new blood vessels which are ordered by diameters and processed later.

As source-list is empty, all the possible blood vessels are detected, and the whole process ends.

## 2.3 Bayesian method for vessel segmentation

During the tracking process, new vessel edge points are obtained based on the probabilities of different configurations. With Bayesian rules, the probability of a configuration at iteration $k$ is described as:

$$P(\chi|Y_k) = \frac{P(Y_k|\chi) \cdot P(\chi)}{P(Y_k)} \tag{2}$$

$\chi$ is the configuration and $Y_k = \{y_s^{(k)}, s = 1,2 \ldots N_k\}$ is the discrete grey level profile relative to the $N_k$ points on semi-ellipse $C_k$. $P(Y_k)$ does not depend on the configuration and will be disregarded. The best configuration is obtained as:

$$\hat{\chi} = \arg\max\{P(Y_k|\chi) \cdot P(\chi)\} \tag{3}$$

### *2.3.1 Likelihood function*

In this study, conditional probability model is assumed to describe the variability of a pixel value on a semi-ellipse $C$ belonging either to the background or to the blood vessel. The background is assumed to have a constant intensity with zero mean additive Gaussian white noise. The grey level profile of the cross section of a blood vessel is approximated as a Gaussian shaped curve with the same Gaussian noise as the background (see Fig.4).

At iteration $k$, considering the case of a normal configuration $\chi$, two corresponding edge points $M_m$ and $M_n$ are the $m^{th}$ and $n^{th}$ points on $C_k$. If $y_i$ is the grey level of $M_i$, the $i^{th}$ point on $C_k$, conditional probability has the general form:

$$P(y_i|\chi) = \frac{1}{\sqrt{2\pi}\sigma} \exp(-\frac{(y_i - \mu_i)^2}{2\sigma^2}) \tag{4}$$

where $\sigma$ is the standard deviation of the additive Gaussian noise, which can be obtained from local background. When $i \in [1, m[ \bigcup ]n, N_k]$, $M_i$ is a point on the background and $\mu_i$ is

equal to $\mu_b$, the mean intensity of local background. When $i \in [m,n]$, $M_i$ is a point inside the vessel. $\mu_i$ can be mathematically expressed as: $\mu_i = K\exp(-\frac{l_i^2}{2\sigma_i^2}) + \mu_b$. $l_i$ is the distance between $M_i$ and the middle point of $[M_m, M_n]$. $\sigma_i$ defines the spread of the sectional intensity profile. In this study, $\sigma_i = \frac{1}{2}|M_m M_n|$. Parameter $K = \mu_v - \mu_b$, $\mu_v$ is the maximum grey level inside the blood vessel in current detection area.

Assuming all these conditional probabilities independent, the likelihood function $P(Y_k|\chi)$ is described as:

$$P(Y_k|\chi) = \prod_{i=1}^{N_k} P(y_i|\chi) = \frac{1}{(\sqrt{2\pi}\sigma)^{N_k}} \exp(-\frac{1}{2\sigma^2}\sum_{i=1}^{N_k}(y_i - \mu_i)^2) \quad (5)$$

For the case of bifurcation or crossing, the likelihood function has a similar form.

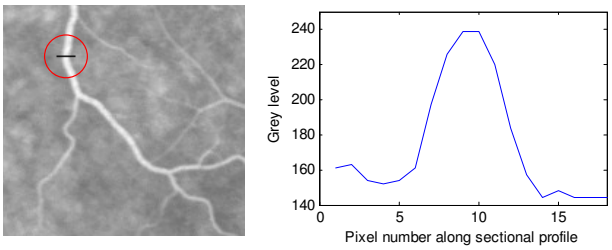


Figure 4: The cross section of a blood vessel

### 2.3.2 *A priori probability*

The *a priori* probability of a configuration $\chi$ is expressed on the basis of Gibbs formulation [16], [17]:

$$P(\chi) = \frac{1}{Z}\exp(-\lambda U(\chi)) \quad (6)$$

where $Z$ is a normalization parameter and $\lambda$ is a weighting factor called regularization term. $U(\chi)$ is the energy associated with the configuration $\chi$. The aim of using Gibbs formulation is to link a configuration with an energy function which penalizes high energetic configurations.

In our study, blood vessels are assumed to be locally linear. At a given step, local vessel edges can be estimated as two straight lines. So the configuration whose candidate edge points are aligned on current edge line is promoted. At iteration $k$ ($k \leq 5$), define $L_1$ and $L_2$ as the straight lines through edge points $\hat{U}_k$ and $\hat{V}_k$ respectively and along local direction $\overrightarrow{D_k}$. When $k > 5$, $L_1$ and $L_2$ are the least square straight lines obtained based on five previous detected points (see Fig.5). $M_m$ and $M_n$ are two edge point candidates of $\chi$. $d_1$ and $d_2$ denote the distance between $L_1$ and $M_m$ and between $L_2$ and $M_n$ respectively. Then energy $U(\chi)$ can be defined as: $U(\chi) = d_1^2 + d_2^2$. *A priori* probability has the expression:

$$P(\chi) = \frac{1}{Z}\exp(-\lambda(d_1^2 + d_2^2)) \quad (7)$$

Finally, according to Eq.3, the configuration which has the maximum value of $P(Y_k|\chi)\cdot P(\chi)$ will be chosen. New edge points will be obtained based on this configuration.

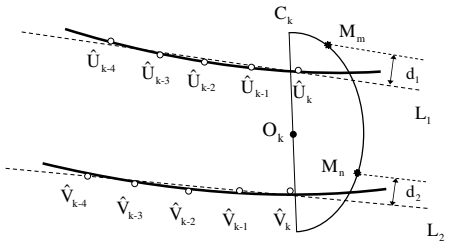


Figure 5: Least square lines

## 3. EXPERIMENTS AND PERFORMANCE EVALUATION

The performance of our algorithm is evaluated on both synthetic and retinal images. Synthetic image is obtained from a noise-free simulated vascular image, which will be used as the true image later. It represents six kinds of vessel segments with different geometries to model different vessel features in retinal images (diameter between 3 and 10 pixels, average grey level 116). Sectional grey levels of these vessel segments are assumed to follow Gaussian distribution [18]. We add white noise on the simulated vascular image to evaluate our algorithm. We use a quality parameter, Segmentation Matching Factor (SMF) [13], to characterize the algorithm performance.

$$SMF = \frac{Card(A_{sim} \bigcap A_{seg})}{Card(A_{sim} \bigcup A_{seg})} \quad (8)$$

where $A_{sim}$ and $A_{seg}$ are the sets of pixels belonging to the simulated and the segmented arterial tree respectively. $Card(A)$ is the number of elements in set $A$. SMF equals 1 in the case of a perfect segmentation, 0 if segmentation fails.

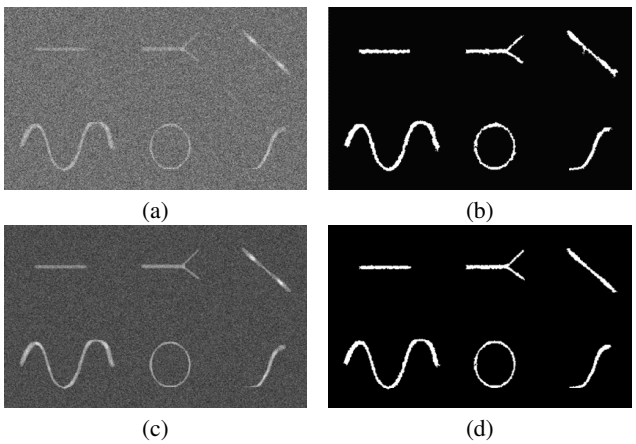


Figure 6: Result on simulated images: (a) and (b) are noisy image ($SNR = 3dB$) and its resulting image after segmentation and reconstruction ($SMF = 0.83$); (c) and (d) are noisy image ($SNR = 10dB$) and its resulting image ($SMF = 0.91$)

Firstly, the influence of noise upon quality parameter SMF was tested. We find that the best SMF was obtained when weighting factor $\lambda$ was 0.01 for all the cases. Fig.6 gives the test result of proposed algorithm on simulated images. For different given Gaussian noise (SNR from $1dB$ to $15dB$, $\lambda = 0.01$), SMF values of different algorithms were

computed. Fig.7 shows the results on simulated images, using our method, Chaudhuri's method [8], and Adel's method [13]. As it can be noticed, our method gives better results. Efficiency of our method was all the higher when SNR was higher. The SMF value can reach 0.9 when SNR is higher than 12. It falls to 0.8 when SNR is lower than 3.

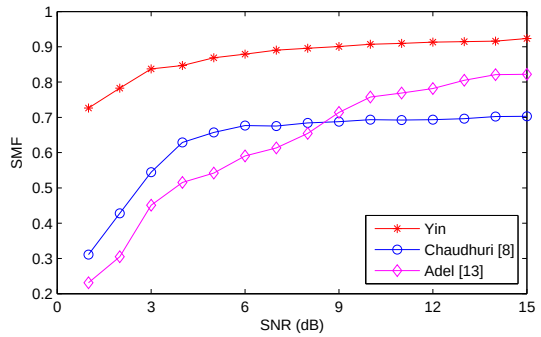


Figure 7: SMF at different SNR's values with $\lambda = 0.01$

On the other hand, we applied our algorithm on retinal images. Fig.8 shows that our algorithm works well and detects different configurations in retinal images. Fig.9 shows the results of our method compared with what was obtained in our previous work [13].

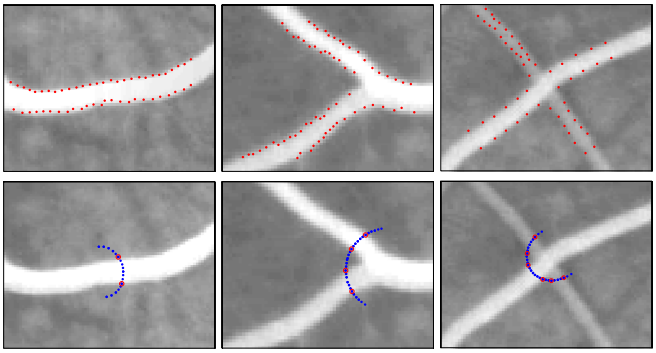

(a) normal (b) bifurcation (c) crossing

Figure 8: Detection of different types of configurations

More tests on retinal images have been done on the publicly available DRIVE database [12]. The database consists of 40 images taken from a screening programme for diabetic retinopathy in the Netherlands. The images have been hand-segmented by three observers: one computer science student, one clinical expert and one image processing expert. We tested our method on 20 images and used the manual segmentation as the "ground truth". For that purpose, subimages were extracted and ROC curves were calculated. The maximum TPR (true positive rate) obtained was 0.82 when corresponding FPR (false positive rate) was 0.01. The FPR did not exceed 0.1 for all experiments.

## 4. CONCLUSION

In this paper, a statistical based tracking method was developed. Vessel edge points are detected based on a Bayesian method using local grey levels statistics and continuity properties of blood vessels. From the experiments and evaluation,

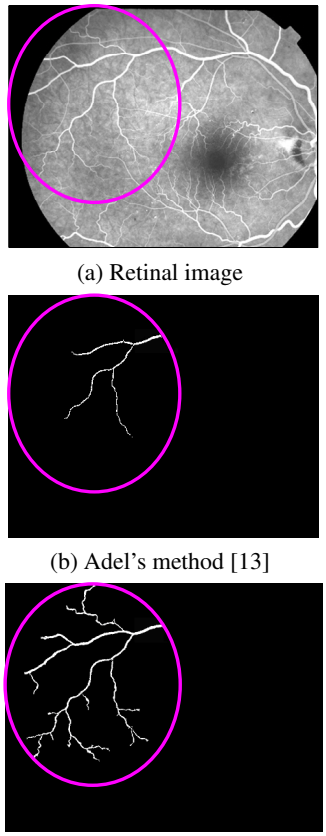

(a) Retinal image

(b) Adel's method [13]

(c) Proposed method

Figure 9: Result on a retinal image

we can see that many improvements have been obtained from our previous work [13], including handling different vessel configurations and improving the robustness against noise. In a near future, a deeper evaluation on retinal images is planed to be carried on to make this method widely usable for vessel tracking algorithm.

## REFERENCES


[1] C. Kirbas and F. Quek, "A review of vessel extraction techniques and algorithms," *ACM Comput. Surv.*, vol. 36, no. 2, pp. 81–121, 2004.

[2] K. Akita and H. Kuga, "A computer method of understanding ocular fundus images," *Pattern Recogn.*, vol. 15, pp. 431–443, 1982.

[3] D.-C. Wu, B. Schwartz, J. Schwoerer, and R. Banwatt, "Retinal blood vessel width measured on color fundus photographs by image analysis," *Acta Ophthalmol. Scand. Suppl.*, vol. 215, pp. 33–40, 1995.

[4] L. Zhou, M. Rzeszotarski, L. Singerman, and J. Chokreff, "The detection and quantification of retinopathy using digital angiograms," *IEEE Trans. Med. Imag.*, vol. 13, pp. 619–626, 1994.

[5] X. Gao, A. Bharath, A. Stanton, A. Hughes, N. Chapman, and S. Thom, "Quantification and characterisation of arteries in retinal images," *Comp. Meth. Program. Biom.*, vol. 63, pp. 133–146, 2000.

[6] Y. Tolias and S. Panas, "A fuzzy vessel tracking al-

gorithm for retinal images based on fuzzy clustering," *IEEE Trans. Med. Imag.*, vol. 17, pp. 263–273, 1998.

[7] X. Jiang and D. Mojon, "Adaptive local thresholding by verificationbased multithreshold probing with application to vessel detection in retinal images," *IEEE Trans. Pattern Recogn. Anal. Mach. Intell.*, vol. 25, pp. 131–137, 2003.

[8] S. Chaudhuri, S. Chatterjee, N. Katz, M. Nelson, and M. Goldbaum, "Detection of blood vessels in retinal images using two-dimensional matched filters," *IEEE Trans. Med. Imag.*, vol. 8, pp. 263–269, 1989.

[9] F. Zana and J. Klein, "Robust segmentation of vessels from retinal angiography," *Proceedings of the International Conference on Digital Signal Processing, Santorini, Greece*, pp. 1087–1090, 1997.

[10] A. Hoover, V. Kouznetsova, and M. Goldbaum, "Locating blood vessels in retinal images by piecewise threshold probing of a matched filter response," *IEEE Trans. Med. Imag.*, vol. 19, pp. 203–210, 2000.

[11] C. Sinthanayothin, J. Boyce, H. Cook, and T. Williamson, "Automated localisation of the optic disc, fovea and retinal blood vessels from digital colour fundus images," *Brit. J. Ophthalmol.*, vol. 83, pp. 902–910, 1999.

[12] J.J. Staal, M.D. Abramoff, M. Niemeijer, M.A. Viergever, and B. van Ginneken, "Ridge-based vessel segmentation in color images of the retina," *IEEE Trans. Med. Imag.*, vol. 23, pp. 501–509, 2004.

[13] M. Adel, M. Rasigni, T. Gaidon, C. Fossati, and S. Bourennane, "Statistical-based linear vessel structure detection in medical images," *IEEE International Conference on Image Processing*, pp. 649–652, 2009.

[14] M. Adel, A. Moussaoui, M. Rasigni, S. Bourennane, and L. Hamami, "Statistical-based tracking technique for linear structures detection: Application to vessel segmentation in medical images," *IEEE Transaction on Signal Processing Letters*, vol. 17, pp. 555–558, 2010.

[15] J. Liu, S. Lu, J.H. Lim, Z. Zhang, T.N. Meng, D.W.K. Wong, and H. Li, "Photometric correction of retinal images by polynomial interpolation," *IEEE International Conference on Image Processing*, pp. 3893–3896, 2009.

[16] M.V. Ibanez and A. Simo, "Bayesian detection of the fovea in eye fundus angiographies," *Pattern Recognition Letters*, vol. 20, pp. 229–240, 1999.

[17] A. Haddouche, M. Adel, M. Rasigni, and S. Bourennane, "Detection of the foveal avascular zone on retinal angiograms using markov random fields," *Digital Signal Processing*, vol. 20, no. 1, pp. 149–154, 2010.

[18] Phan T.H. Truc, Md. A.U. Khan, Young-Koo Lee, Sungyoung Lee, and Tae-Seong Kim, "Vessel enhancement filter using directional filter bank," *Comput. Vis. Image Underst.*, vol. 113, no. 1, pp. 101–112, 2009.